Instabilities in Free-Surface Electroosmotic Flows

Sang W. Joo

Tel.: ++82 (0)53 810 2568; Fax: ++82(0)53 810 4627; Email: swjoo@yu.ac.kr
School of Mechanical Engineering, Yeungnam University, KOREA

Abstract With the recent development of novel microfluidic devices electroosmotic flows with fluid/fluid interfaces have emerged as very important subjects of investigation. Two immiscible fluids may need to be transported in a microchannel, or one side of a channel may be open to air for various purposes, including adsorption of airborne molecules to liquid for high-sensitivity substance detection. The liquid/liquid or liquid/gas interface in these cases can deform, resulting in significant corrugations followed sometimes by incipient rupture of liquid layers. For electroosmotic flow the rupture, leading to shortcircuit, can cause overall failure of the device. It is thus imperative to know the conditions for the rupture as well as the initial interfacial instability. Studies based on the Debye-Huckle approximation reveal that all free-surface electroosmotic flows of thickness larger than the Debye screening length are unstable and selectively lead to rupture. Layers of the order of Debye screening length, however, are not properly described by the Debye-Huckle approximation. Even for micro-scale layers, the rupture phenomenon can make local layer thickness to be nanoscale. A fully coupled system of hydrodynamics, electric field, and ionic distribution need to be analyzed. In this paper linear instability and subsequent nonlinear developments of a nanoscale free-surface electroosmotic flow are reported.
Keywords: Electroosmosis, Free Surface, Instability, Rupture

1. Introduction

With recent development of micro/nanofluidic devices, electro-osmotic flows are studied more intensively than ever, as summarized by (Heeren et al., 2007; Hunter, 1996; Nguyen and Wereley, 2002; Reppert and Morgan, 2002, Li, 2004). In microchannels with cross-sectional hydraulic length scale much larger than the Debye length, a plug flow develops along the core part of the channel with the application of direct-current (DC), while a thin shear layer is formed very near the channel wall. At approximately three Debye lengths from the channel wall, the fluid reaches the core velocity. In such situations, the Poisson-Boltzmann equation or its linearized version for weak surface potemtial, the Debye Hückel approximation, may be sufficient to describe the flow. In nanochannels with the hydraulic length scale comparable to the Debye length, however, the fully coupled system of the continuity and Navier-Stokes equation for the hydrodyanmics, the Poisson equation for the electric potential, and the Nernst-Planck equation for the ionic concentration has to be considered.

New micro/nanofluidic devices often require electroosmotic flows with a new dimension of consideration. A microchannel system may have in part an open channel flow in place of the usual internal flow. Or even a channel-less rivulet may be designed to transport a highly viscous solution by electro-osmosis. In these cases, an interface with the air, or other gaseous phases, exists, and can deform with the flow development. The interface will exist in an internal channel flow as well, if more than one aqueous solutions are transported. At times it may be necessary to feed two different fluids at the same time or to use the electro-osmotic mobility of one fluid to move the other. Studies on electroosmotic flows with deformable interface are relatively scarce. The interface between two macro-scale immiscible liquids driven by other mechanisms are known to be unstable (Alekseenko et al., 1994; Nepomnyaschy et al., 2002), and prone to severe corrugations. It is therefore important to identify interfacialy instabilities in multiphase electroosmotic flows because the electric field and the corresponding ionic distribution will be very sensitive to the shape of the interface. Two-fluid electro-osmotic flows with a free

surface, or an interface, has been investigated in microchannels by Lee and Li (2006), Gao et al. (2005 a, b), Ngoma and Erchiqui (2006) and Gao et al. (2007). However, the interfacial deformations, which are not known a priori, are not taken into account.

A linear interfacial instability in electroosmotic flow is identified by Joo (2007) for a micro-scale liquid layer bounded below by a rigid substratate and above by the air. It is shown that all electroosmotic open flows, based on the Debye Hückel approximation, are susceptible to interfacial instabilities, resulting in free-surface corrugations. Nonlinear development of the free surface beyond the linear instability is subsequently investigated by deriving and numerically integrating an evolution equation for the local film thickness with the lubrication approximation (Joo, 2008). The study shows that the electro-osmotic instability can cause severe free-sruface deformations, leading even to rupture of the layer. Short circuit, and thus complete failure of the electroosmosis, can then be expected.

In the present investigation, the effects of interfacial dynamics are studied for an electro-osmotic flow with and without slip on a substrate. The free surface may deform with flow developments, and can in turn affect the electro-osmotic flow. A linear stability of the basic state with a planar interface is analyzed by superposing a small-amplitude disturbance to the basic state, substituting them into the original unsteady system, and linearizing for small amplitude to obtain an Orr-Sommerfeld eigenvalue problem. The stability bounds beyond which the disturbance grows is obtained by solving the OS eigenvalue problem numerically. The time-dependednt location of the film surface is not known a priori, and imposes nonlinearity in the system. Subsequent nonlinear analysis based on long-wave asysmptotics yields an evolution equation for the local layer film thickness which is solved numerically to understand the transient development of nonlinear waves. Steady state solutions of a fluid spreading over a surface with contact line motion are solved numerically in order to understand the influence of parameters on the film flow system.

2. Problem Statement

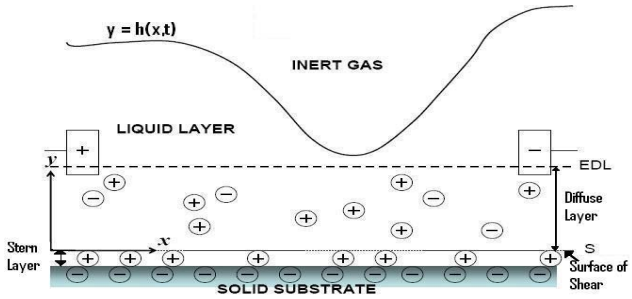

Figure 1 Scheme of electro-osmotic flow with free surface.

The system under consideration consists of the flow of an incompressible thin aqueous film of thickness *d,* with constant density ρ, viscosity μ, surface tension σ flowing on a rigid plane driven by an elctro-osmotic force produced due to the presence of an applied electric field held parallel to the x-axis. It is assumed that the substrate bears a negative charge of zeta potential upon contact with the solution, generating a positively charged electric double layer (EDL), composed of an immobile stern layer and the mobile diffuse layer as shown in Fig. 1. An inert gas bounds the film above and y-axis is normal to the plane. The film flow variables are nondimensionalized choosing *d,* $\rho d^2/\mu$, $\mu/\rho d$ and $\mu^2/\rho d^2$ as scales for length, time, velocity and pressure. Using the above scales, the components of Navier-Stokes equation are

$$u_t + uu_x + vu_y = -\left(p + \frac{A}{h^3}\right)_x + u_{xx} + u_{yy} + \frac{Eo}{De^2} e^{-y/De}$$

$$v_t + uv_x + vv_y = -p_y + v_{xx} + v_{yy} \qquad (1)$$

where $A = \frac{a\rho}{d\mu^2}$ measures the unretarded London-van der Waals attraction, *a* being the Hamaker constant. The parameter $Eo = \frac{\sum E_{el}\zeta d\rho}{\mu^2}$ is the elctro-osmosis number which measures the applied electrical field strength E_{el}, where ζ is the zeta potential

prescribed at the line of shear and Σ is a dielectric constant. The Debye number $De = \frac{\lambda_d}{d}$ measures the Debye length relative to the mean thickness of the liquid layer where λ_d is the Debye length of the electrolyte solution. The continuity equation for an incompressible fluid conserves mass and the flow is subject to the usual no-slip condition along the rigid substrate (y = 0). Along the interface ($y = h(x,t)$), the normal and tangential stress conditions are given by

$$-p + \frac{2}{N^2}\left[u_x\left(h_x{}^2 - 1\right) - h_x\left(u_y + v_x\right)\right] = \frac{S}{N^3}h_{xx} \quad (2)$$

$$\left(u_y + v_x\right)\left(1 - h_x{}^2\right) - 4u_x h_x = 0 \quad (3)$$

where $N = \sqrt{1 + h_x{}^2}$, and $S = \frac{\sigma d\rho}{\mu^2}$ is the dimensionless surface tension parameter. Finally, the interface is governed by the kinematic boundary condition expressing that the free surface is a material surface, that is

$$v = h_t + uh_x . \quad (4)$$

3. Linear Stability Analysis

When the flow is stationary, of constant film thickness h = 1, the solution of the Navier-Stokes equation is a parallel flow given by

$$U(y) = Eo\left(1 - e^{-y/De} - \frac{y}{De}e^{-1/De}\right),\ V(y) = 0$$

and $P(y)$ = 0 (Joo, 2007). The linear stability of the film flow system is analyzed by perturbing primary flow with respect to infinitesimal disturbances and linearizing the equations. The pressure disturbance is eliminated from the linearized disturbance equations, and the velocity disturbance is expressed in terms of the stream function given by

$$\hat{u} = \psi_y \ \hat{v} = -\psi_x \quad (5)$$

Introducing the normal mode $\psi = \phi(y)e^{i(kx-ct)}$, where k is the real wave number and c is complex growth rate, into the resulting stream function disturbance equation we obtain the Orr-Sommerfeld eigenvalue problem given by

$$\left(D^2 - k^2\right)^2\phi + ik\left[(c-U)\left(D^2 - k^2\right) + D^2U\right]\phi = 0 \quad (6)$$

The boundary conditions become

$$\phi(0) = 0 \quad \phi'(0) = 0 \quad (7)$$

$$\left(D^2 - 3k^2\right)D\phi(1) + ik\left(c - U(1)\right)D\phi(1) = i\eta k\left(-3A + Sk^2\right) \quad (8)$$

$$\left(D^2 + k^2\right)\phi(1) + D^2U(1)\eta = 0 \quad (9)$$

$$\phi(1) = \eta\left(c - U(1)\right) \quad (10)$$

where $D \equiv d/dy$, and the values of the parameter c that lead to a non-trivial solution provide the relationship between the conditions of the primary flow and the evolution of various disturbance modes. For disturbance of waves whose wavelength is large compared to the mean film thickness, the interfacial instability due to electro-osmotic flow can be studied theoretically. In terms of long-wavelength asymptotics, solution of the eigenvalue problem is obtained by considering an expansion of the eigenfunction ϕ and the eigenvalue c around their solutions for k = 0 as

$$c = c_0 + ikc_1 - k^2c_2 - ik^3c_3$$

$$\phi = \phi_0 + ik\phi_1 - k^2\phi_2 - ik^3\phi_3 \quad (11)$$

following the method proposed by Yih (1963). The results for the complex phase speed are obtained as

$$c_0 = E_0 - E_0\left(1 + 1/De - 1/\left(2De^2\right)\right)e^{-1/De}$$

$$c_1 = A + \left(5De - 9De^4\right)Eo^2e^{-1/De} + \left(\frac{5Eo^2}{48De^4} - \frac{2Eo^2}{15De^3} - \frac{11Eo^2}{24De^2} - \frac{Eo^2}{2} - \frac{Eo^2}{De} + 4DeEo^2 + 9Eo^2De^2\right)e^{-2/De}$$

$$c_3 = \frac{S}{3} + \text{other terms} \quad (12)$$

Equations (12) represent an exact asymptotic result which could be compared with simple asymptotic models. The surface tension parameter appears only at the order three in the k- expansion. However, the surface tension is the only physical effect that limits the growth rate of short waves ($k \to 0$) and then prevents waves from breaking. It implies that $k^2S = O(1)$ when k corresponds to waves observed

experimentally in the flow of a thin liquid film (Aleekseenko, 1994). In this case, the marginal stability curve corresponding to a zero growth rate can be obtained close to the criticality by truncating the long-wavelength expansion (12) at lowest order in k:

$$\left(5De-9De^4\right)Eo^2e^{-1/De}+\left(\begin{array}{l}\frac{5Eo^2}{48De^4}-\frac{2Eo^2}{15De^3}-\frac{11Eo^2}{24De^2}\\-\frac{Eo^2}{2}-\frac{Eo^2}{De}+4DeEo^2+9Eo^2De^2\end{array}\right)e^{-2/De}$$

$$=\frac{k_c{}^2S}{3}-A \qquad (13)$$

where k_c is the cut-off wave number. Equation (13) describes the locus of points where the growth rate is zero. It is to be noted that the wave number $k_m=\frac{k_c}{\sqrt{2}}$, corresponding to maximal growth rate is obtained from the relation $\frac{\partial\left(k\,\mathrm{Im}(c)\right)}{\partial k}=0.$

4. Long-Wave Asymptotics

The main issue of this work is to study the dynamics of a thin film electro-osmotic flow, where long-wave instability modes are dominant. Therefore, an approximation arising from the smallness of the film thickness modulations as compared to the film thickness itself is applied. In the boundary layer theory, the strong viscous diffusion in the cross-stream y component of the momentum equation ensues the coherence of the flow across the momentum boundary layer whose thickness is a solution of the problem. The flow is laminar in the core of the viscous boundary layer and the inertia terms associated to the fluid motion along the y-coordinate can be neglected. Thin viscous film flows share the same characteristics such that boundary layer theory applies, but only as an approximation since the film thickness is *a priori* determined by the flow rate.

To express that the slope of the interface is always small with regards to the film thickness itself, a formal film parameter $\varepsilon << 1$ is introduced. Practically it consists of applying a gradient expansion through the transformation $\partial_t\to\varepsilon\partial_t,\partial_x\to\varepsilon\partial_x$ and $v\to\varepsilon v$. Accomplishing this transformation in the system (1)-(4) together with the mass balance condition and the no-slip condition at the interface, an equation for the evolution of local film thickness is obtained following the method proposed by Benney (1966) as

$$h_t+\ddot{A}(h)h_x+\varepsilon\frac{\partial}{\partial x}\left(\ddot{B}(h)h_x+\ddot{C}(h)h_{xxx}\right)=0\,(14)$$

where =

$$\ddot{A}(h)=Eo+e^{-h/De}\left(-Eo-\frac{Eoh}{De}+\frac{Eoh^2}{2De^2}\right)$$

$$\ddot{B}(h)=\frac{A}{h}+e^{-h/De}Eo^2\left(5hDe-9De^2\right)+e^{-2h/De}Eo^2$$

$$\left(\frac{5h^6}{48De^4}-\frac{2h^5}{15De^3}-\frac{11h^4}{24De^2}-\frac{h^3}{De}-\frac{h^2}{2}+4hDe+9De^2\right)$$

$$\ddot{C}(h)=\frac{Sh^3}{3}.$$

The first term in Benney type equation given by (14) describes wave propagation and steepening effects. The second term in it represents the destabilizing effects of van der Waals attraction and electro-osmotic force, while the third term corresponds to the stabilizing capillary effects.

5. Stability Analysis

In order to investigate the stability characteristics of the power-law film, it is convenient to separate the time-averaged and the disturbance (unsteady) components of the film thickness so that $h(x,t)=H_0(x)+H(x,t)$ where $H_0(x)$ *is* the time averaged part of the film thickness and $H(x,t)$ is the unsteady part of the film thickness representing the disturbance component. If the variation of film thickness for the base flow is very small ε ,(i.e. $\left|\varepsilon H_0(x)\right|<<1$), then, it is reasonable to neglect the derivatives of the average film thickness with respect to x in the unsteady equation and this simplification corresponds to parallel flow approximation.

Further, by letting $H_0 = 1$ in the unsteady equation, which implies that the unsteady equation is only locally valid, the unsteady wave equation is obtained as

$$H_t + A_1 H_x + \varepsilon B_1 H_{xx} + \varepsilon C_1 H_{xxx} =$$
$$-\left[A_1' H + \frac{A_1'' H^2}{2} \right] H_x - \varepsilon \left[B_1' H + \frac{B_1'' H^2}{2} \right] H_{xx}$$
$$- \varepsilon \left[C_1' H + \frac{C_1'' H^2}{2} \right] H_{xxx}$$

$$- \varepsilon \left[B_1' + B_1'' H \right] H_x{}^2 - \varepsilon \left[C_1' + C_1'' H \right] H_x H_{xxx}$$
$$+ O\left(H^4\right) \qquad (15)$$

where

$$A_1 = \ddot{A}(h=1), A_1' = \ddot{A}'(h=1), A_1'' = \ddot{A}''(h=1) \ ;$$
$$B_1 = \ddot{B}(h=1), B' = \ddot{B}'(h=1), B_1'' = \ddot{B}''(h=1)$$

etc., and the prime denotes derivative with respect to h.

5.1 Linear Stability of Long-wave Equation

Considering linear terms in (15) alone, and assuming the normal mode solution as

$$H = \Gamma e^{i(kx - c_L t) + st} + \Gamma e^{-i(kx - c_L t) - st} \qquad (16)$$

where $\Gamma << 1$, k, c_L and s are real and represent the amplitude, the wavenumber, linear phase speed and the linear growth rate of the disturbance, the expression for growth rate and phase speed are obtained as

$$c_L = E_0 - E_0\left(1 + 1/De - 1/\left(2De^2\right)\right) e^{-1/De}$$
$$s = A + \left(5De - 9De^4\right) Eo^2 e^{-1/De} +$$
$$\left(\frac{5Eo^2}{48De^4} - \frac{2Eo^2}{15De^3} - \frac{11Eo^2}{24De^2} - \frac{Eo^2}{2} \right) e^{-2/De} - \frac{k^2 S}{3}$$
$$\left(- \frac{Eo^2}{De} + 4DeEo^2 + 9Eo^2 De^2 \right)$$

It should be noted that the relation $s = 0$, yields the relation (13). When $s > 0$, the film flow is unstable where as the flow is stable if $s < 0$.

5.2 Nonlinear Stability Analysis of Long-wave Equation

Linear theory fails in capturing the flow behavior accurately as the perturbed waves grow to a finite amplitude. In order to examine whether the nonlinear wave in the vicinity of criticality attains a finite amplitude and remains stable or continues to grow in time to become unstable, a weakly nonlinear stability analysis is performed. The nonlinear stability analysis of (15) by the method of multiple scales (Oron and Gottleib, 2004; Sadiq, 2007) yields the threshold amplitude $\alpha\Gamma_0$ and the nonlinear wave speed N_c as (α measures distance from criticality)

$$\alpha\Gamma_0 = \sqrt{\frac{s}{J_2}} \quad N_c = c + s\frac{J_4}{J_2} \qquad (17)$$

where

$$J_2 = \varepsilon\left(7k^4 e_r C_1' - k^2 e_r B_1' - \frac{k^2}{2} B_1'' + \frac{k^4}{2} C_1'' \right)$$
$$- k e_i A_1' ; J_4 = \varepsilon\left(7k^4 e_i C_1' - k^2 e_i B_1' \right) + k e_r A_1' + k \frac{A_1''}{2}$$

$$e_r = \frac{2\left(B_1' - k^2 C_1' \right)}{\left(-4B_1 + 16k^2 C_1 \right)} ; e_i = \frac{-A_1'}{\varepsilon\left(-4kB_1 + 16k^3 C_1 \right)}.$$

It is observed from (17) that in the linear unstable region $s > 0$, the condition for existence of a supercritical stable region is $J_2 > 0$ and $\alpha\Gamma_0$ is the threshold amplitude. In the linear stable region $s < 0$, if $J_2 < 0$, then the flow has the behaviour of subcritical instability and $\alpha\Gamma_0$ is the threshold amplitude. The condition for the existence of a subcritical stable region is $s < 0$, $J_2 > 0$ and $J_2 = 0$ gives the condition of existence of a neutral stability curve. It is also observed from (17) that a negative value of J_2 can make the system unstable. In this case, if $s > 0$ then the amplitude of the disturbance may become larger than the threshold amplitude and cause the system to reach an explosive state. This analysis although qualitatively predicts the behaviour of phase speed and threshold amplitude of nonlinear waves, the transient

development of waves is better understood by solving the evolution equation (14) numerically in a periodic domain (Joo, 2008) considering it as an initial value problem with $h(x,0) = 1 - \cos(kx)$ to be an initial value. The numerical experiment for the evolution of finite amplitude perturbations clarifies the mechanism responsible for the transfer of energy from the basic state to the disturbance.

5.3 Results and Discussion

The marginal stability curves are obtained by solving the Orr-Sommerfeld system numerically. The OS system is a complex ODE of degree four for the amplitude of the perturbed cross-stream velocity and subject to four boundary conditions. As the differential equation is linear, an integral constraint viz, $\int_0^1 \phi(y)dy = 1$ is also considered for solving the OS system (6)-(10). The system is recast into a dynamical system of dimension four and subject to the above integral constraint. The solution branches were constructed by continuation starting from the trivial zero-wavenumber solution. AUTO97 (Doedel, 1977) was used for accomplishing the above task by adopting Keller's pseudo-arclength continuation method. The numerical curves were compared with the curves obtained through the dispersion relation (13) as a check.

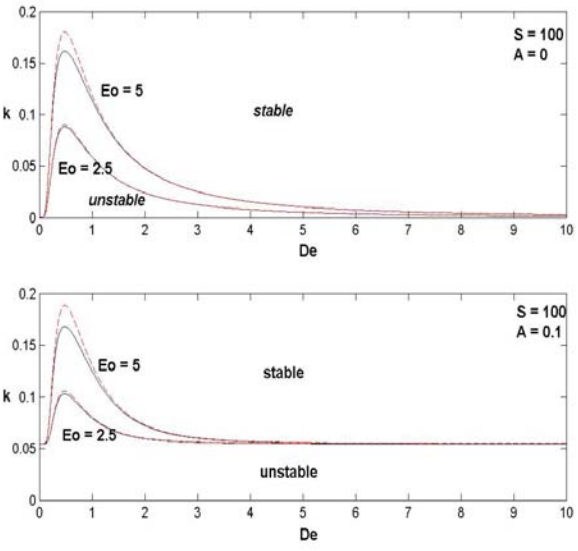

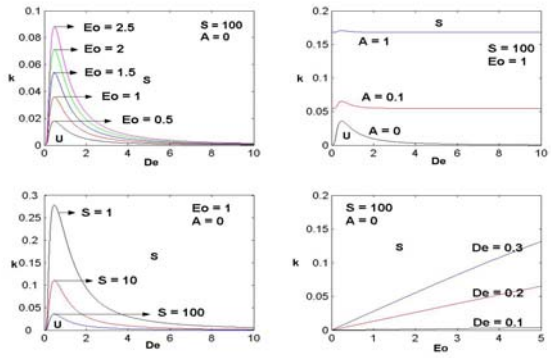

Figure 2: Marginal stability curves. Solid lines are curves obtained through OS system and and dashed lines are curves yielded through the dispersion relation.

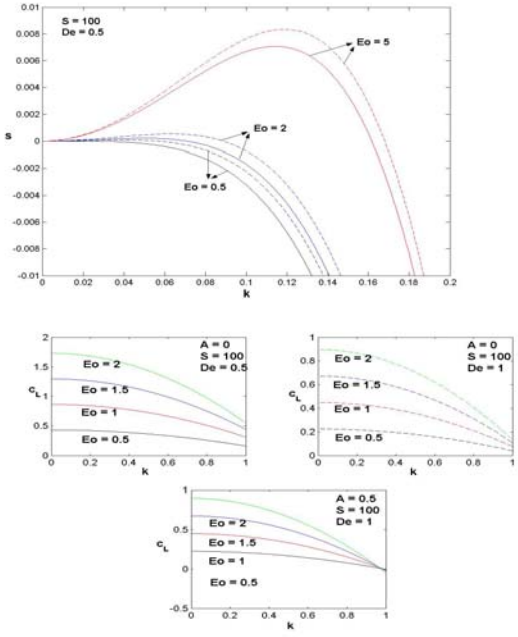

Figure 3: Growth rate and phase speed of nonlinear waves. Solid lines are for $A = 0$ and dashed lines are for $A = 0.1$.

Neutral stability curves for various parametric effects are displayed in Fig. 2. The stability curves divide the *k-De* plane into stable and unstable flow domains. It is seen that OS curves agree qualitatively with the curves yielded through the dispersion relation (13). With increase in applied electrical field strength, the instability enhances in general. The marginal stability curves originate at a finite distance above origin when van der Waals effect is included. This is primarily due to the reason that as $De \to 0$, k does not vanish for non-zero A (see condition (13)). It is

observed that the band of unstable wavenumbers increases with increase in the magnitude of van der Waals attraction. As a function of *Eo,* the unstable region increases up to a specific small value of *De* and after which a reverse trend is observed. This is also seen from the figures displayed to the left in Fig. 2. For small values of *De*, the flow is more unstable. For values of *De* of *O*(1), there exists a constant critical wavenumber above which the flow is stable and below which the film is unstable. Also, it is observed that increase in capillary effects (*S*) stabilizes the system. The growth rate curves and phase speed of linear waves as a function of wavenumber are shown in Fig. 3. The growth rate increases with increase in both *Eo* and van der Waals attraction. There exists a critical *k* below which the growth rate increases and above which it decreases. The phase speed curves displayed in Fig. 3 reveal that the phase speed increases with increase in electrical field strength. As a function of *k*, the phase speed decreases and a similar analogous behaviour is also observed with increase in Debye number.

The friction offered by the fluid against the flow diminishes with increase in applied electrical field strength. The growth rate increases and the phase speed of waves decreases, as a cause the flow becomes more susceptible to disturbances with subsequent increase in instability threshold.

Supercritical stable ($s > 0$, $J_2 > 0$) and subcritical unstable ($s < 0$, $J_2 < 0$) regions where nonlinear waves with finite amplitude exist are shown in Fig. 4 and it is observed that supercritical stable region increases with increase in the value of *Eo* and *A*. The threshold amplitude of nonlinear waves as a function of wavenumber is displayed at the right in Fig. 4 and is observed that the amplitude of nonlinear waves become smaller as *De* increases. The solid curves in the figure are for *Eo* = 1 and the dashed curves are for *Eo* = 2., which shows that increase in the magnitude of *Eo* increases the height of the amplitude when zero van der Waals effect is not considered. However, with the presence of van der Waals effect, the amplitude of waves decreases with

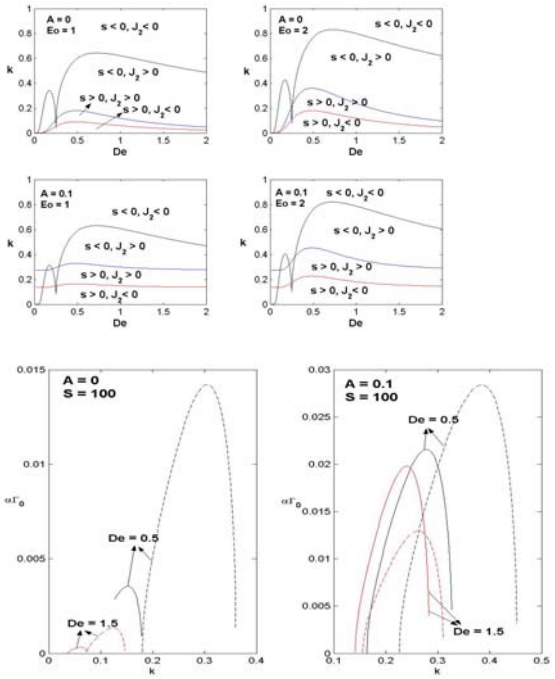

Figure 4: Existence of finite amplitude regions and threshold amplitude of nonlinear waves in supercritical stable region for $\varepsilon = 0.2$.

increase in the value of both *Eo* and *De* but remains larger compared to the $A = 0$ case. It is also infered from the figure that there exist a critical *k* below which threshold amplitude increase and above which it decreases.

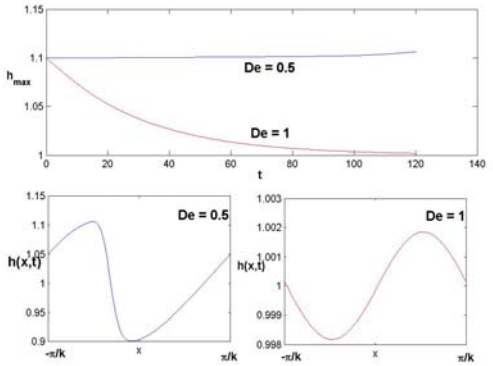

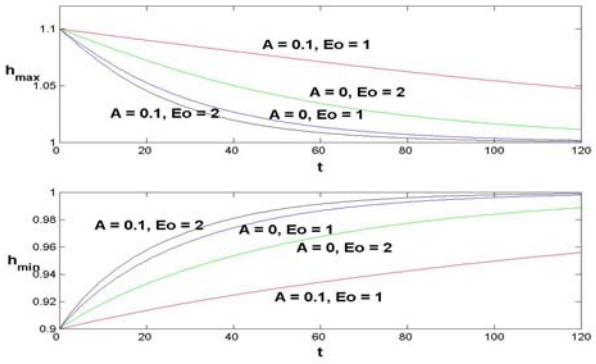

Figure 5: Maxmimum amplitude and surface wave instability of the film flow system corresponding to *S= 100, ε = 0.2* shown at the left for *Eo* = 1 and the amplitude profiles of nonlinear waves are shown at the right.

Numerical experiment of the nonlinear evolution equation for film thickness solved in a periodic domain (Joo, 2008) using finite difference scheme confirms the theoretical predictions established in Fig. 4 through weakly nonlinear analysis and through the curves obtained using the dispersion relation (13). In accordance to the findings reported in the above paragraph, it is seen that for an increase in the value of *Eo*, the amplitude of the waves increases when *A* = 0. However, an opposite trend is observed with siginificant increase in *A* value for the curves displayed at right corresponding to *De* = 1. It is also observed that with an increase in the Debye number magnitude, the maximum amplitude of waves and surface wave instability decrease as shown in the figure at the left. This result agrees with the Orr-Sommerfeld prediction established in Fig. 2.

Thin electro-osmotic film flow is also susceptible to rupture in certain parametric limits as has been reported earlier (Joo, 2008). Such an investigation is neglected here in order to avoid repetition. The present investigation quantifies the results obtained through Orr-Sommerfeld analysis with the curves predicted through weakly nonlinear behaviour of waves both by theoretical and numerical approach which has not been addressed earlier for film flow on rigid planes.

6. Electro-Osmotic flow with slip

The dynamics of contact line in industrial processes involving coating of a thin viscous sheet on a solid surface is a subject of substantial fundamental and technological importance. In microfluidic devices, situations may arise where liquid with deformable surface must be transported by electro-osmosis when there is a presence of contact line motion.

In this section, steady-state solutions of a coating thin liquid film driven by electro-osmosis and van der Waals force with contact line movement along a substrate moving with constant velocity and no spanwise variations are sought using Chebyshev pseudo-spectral method from a nonlinear evolution equation derived under lubrication assumption. The equations of motion and boundary conditions for which are exactly the same as presented above for an electro-osmotic force driven film flow on a rigid plane except for the fact that slip is allowed at the rigid surface. A Navier-type slip condition along the solid interface is used in order to avoid stress singularity at the contact line given by $u = \frac{\lambda}{h} u_y, v = 0$ where $\lambda = \frac{\hat{\lambda}}{d^2}$ (Sadiq and Usha, 2006). Using long-wave asymptotics, the evolution equation for such a film flow is similar to (14) with the terms now being

$$\hat{A}(h) = \ddot{A}(h) - \frac{\lambda Eo}{De^2} e^{-h/De}$$

$$\hat{B}(h) = \ddot{B}(h) + \lambda^3 \left[\left(\frac{1}{De^4} + \frac{2}{hDe^3} + \frac{1}{h^2 De^2} \right) h_x Eo^2 e^{-2h/De} + \frac{Eo^2 h_x}{h^2 De^2} - \left(\frac{2Eo^2}{hDe^3} + \frac{2Eo^2}{h^2 De^2} \right) h_x e^{-h/De} \right] + \lambda^2 \times$$

$$\left[\left(\frac{4h^2}{3De^4} + \frac{2h}{3De^3} - \frac{8}{3De^2} - \frac{4}{hDe} - \frac{2}{h^2} \right) h_x Eo^2 e^{-2h/De} + \left(\frac{1}{3De^2} - \frac{5h}{3De^3} + \frac{4}{hDe} + \frac{4}{h^2} \right) h_x Eo^2 e^{-h/De} \right] + \lambda \times$$

$$\left[\left(\frac{5h^4}{8De^4}-\frac{7h^3}{24De^3}-\frac{13h^2}{6De^2}-\frac{23h}{6De}-2+\frac{5De}{h}+\frac{4De^2}{h^2}\right)h_x-\frac{3h^3}{De}+\frac{h^2}{De}+\frac{5h}{De}+6-\frac{2De}{h}\right.$$

$$\left.-\frac{8De^2}{h^2})h_x Eo^2 e^{-h/De}+\left(\frac{4De^2}{h^2}-\frac{3De}{h}\right)Eo^2 h_x{}^2\right]$$

$\hat{C}(h)=\ddot{C}(h)+(\varepsilon^2 S)\lambda h h_{xxx}$ where $\ddot{A}(h),\ddot{B}(h)$ and $\ddot{C}(h)$ corresponds to terms in (14).

The steady-state solutions which move down along the substrate at a constant velocity $c = 1$ and with no spanwise variations are determined by setting $a(t)\rightarrow a_0(t)$, where $a(t)$ corresponds to the location of contact line. The inertial frame with origin at the contact line is given by the transformation $\xi = x - a_0(t)$, $\tau = t$ and $h(x,t) \rightarrow h_0(\xi)$ (Sadiq and Usha, 2006). The steady-state interface thickness which corresponds to the balance between surface tension force, van der Waals effect, Debye number and the electrical field strength is determined by solving the following ordinary differential equation

$$-\dot{a}_0(t)+\hat{A}(1)+\varepsilon\hat{B}(1)h_0'+\varepsilon\hat{C}(1)h_0'''=0 \qquad (18)$$

where $\dot{a}_0=\hat{A}(1)$. The boundary conditions at the contact line are $h_0(0)=0; h_0'(0)=-\left(\theta_s+D\dot{a}_0{}^{1/m}\right)$ and $h_0(\xi\rightarrow-\infty)=1$ where Θ_s =0.6 is the static contact angle, m=1 and D =1 (Sadiq and Usha, 2006).

The steady state profiles computed numerically (Sadiq and Usha, 2006) are presented in Fig. 6. For a fixed *De*, it is observed that the hump of the profile increases against hydrostatic effects with increase in the value *Eo*. For *Eo* at *O*(1) values, the steady state is almost zero near the contact line for *A*=0. With the presence of van der Waals effect, the film tends to rupture with siginificant increase in the magnitude of *Eo* value as shown in Fig. 6. It is also seen that increase in the value of *De* causes the height of steady-state profile to reach almost zero value with (not shown here) and without van der Waals effect.

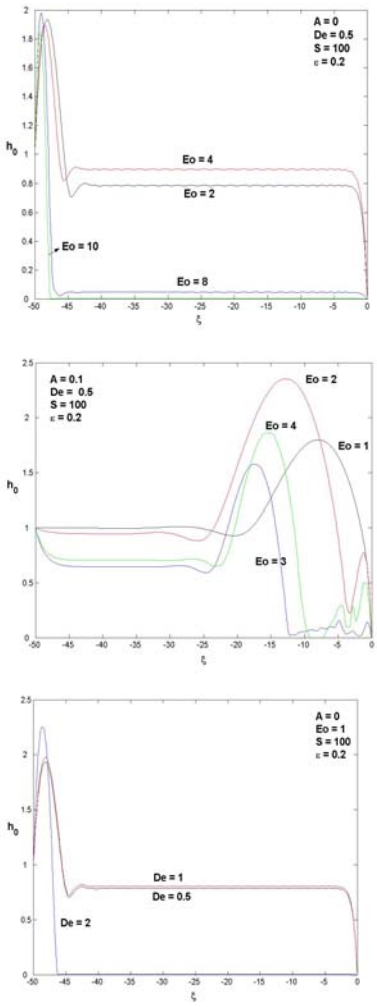

Figure 6: Steady state profiles for a thin film electro-osmotic flow with contact line movement.

7. Conclusions

The problem on electro-osmotically driven thin liquid film with/without van der Waals effect is studied under lubrication assumption for flows based on Debye-Hückel approximation. The Orr-Sommerfeld analysis results agreed qualitatively well with leading order asymptotic theory and numerical predictions. The steady state profile in the presence of contact line movement revelaed the behaviour of rupture of the film as had been reported in Joo (2008). Increasing the magnitude of applied electrical field and Debye number are the main cause of the instability. The viscosity at the bottom reduces with increased electrical field strength and the

liquid loses its resistance against the flow to become unstable.

A more rigorous analysis with the fully coupled system, modeling layer thickness comparable to the Debye length, was performed, and will be presented.

Acknowledgements

This study is sponsored by the Ministry of Education, Science and Technology of Korea through the World Class University Grant.

References

[1] Reuss, F. F. (1809). Charged induced flow. *Proceedings of the Imperial Society of Naturalists of Moscow,* **3**, 327-344.
[2] Hunter, R. J. (1996). *Introduction to modern colloid science*. Oxford University Press, New York.
[3] Nguyen, N. T., & Wereley, S. T. (2002). *Fundamentals and applications of microfluidics*. Artech House, London.
[4] Reppert, P. M., & Morgan, F. D. (2002). Frequency dependent electroosmosis. *J. Colloin Interface Sci.* **7**, 372-383.
[5] Li, D. (2004). *Electokinetics in microfluidics*. Elsevier, Amsterdam.
[6] Alekseenko, S. V., Nakoryakov, V. E., & Pokusaev, B. G. (1994). *Wave flow in liquid films*: third ed. Begell House, New York.
[7] Nepomnyaschy, A. A., Velarde, M. G., & Colinet, P. (2002). *Interfacial phenomena and convection*. Chapman & Hall/CRC.
[8] Lee, J. S. H., & Li, D. (2006). Electro-osmotic flow at a liquid-air interface. *Microfluid Nanofluid*, **2**, 361-365.
[9] Gao, Y., Wong,, T. N., Chai, J. C., Yang, C., & Ooi, K. T. (2005a). Numerical simulation of two-fluid electro-osmotic flow in microchannels. *Int. J. Heat Mass Transfer*. **48**, 5103-5111.
[10] Gao, Y., Wong,, T. N., Yang, C., & Ooi, K. T. (2005b). Two-fluid electro-osmotic flow in microchannels. *J. Colloin Interface Sci.* **284**, 306-314.
[11] Ngoma, G. D., & Erchiqui, F. (2006) . Presuusre gradient and electroosmotic effects on two immicible fluids in a microchannel between two parallel plates. *J. Micromech. Microeng.***16**, 83-91.
[12] Gao, Y., Wang, C., Wong,, T. N., Yang, C., Nguyen, N. T. & Ooi, K. T. (2007). Electroosmotic control of the interface position of two-fluid flow through a microchannel. *J. Micromech. Microeng.***17**, 358-366.
[13] Joo, S. W. (2007). A new hydrodynamic instability in ultra-thin film flows induced by electro-osmosis. *J.Mech.Sci.Tech.***22**, 382-386.
[14] Joo, S.W. (2008). A nonlinear study on the interfacial instabilities in electro-osmotic flows based on the Debye-Hückel approximation. *Microfluidics Nanofluidics*. DOI 10.1007/s10404-008-0262-z.
[15] Benney, D. J. (1966). Long waves on liquid films. *J.Math.Phys.***45**, 150-155.
[16] Oron, A., & Gottleib, O. (2004). Subcritical and supercritical bifurcations of the first- and second-order Benney equations. *J. Engineering Mathematics*. **50**, 121-140.
[17] Sadiq, I. M. R. (2007). *Thin liquid film flow and instability*. Ph.D Thesis, IIT Madras, India.
[18] Doedel, E., Champneys, A., Fairfrieve, T., Kuznetsov, Y., Sandstede, B., & Wang. X. (1997). Auto 97 Continuation and bifurcation software for ordinary differential equations.
[19] Sadiq, I. M. R., & Usha, R. (2006) Spreading of a thin-film of a power-law liquid on an inclined plane: Contact line motion. *Proceedings of the International conference on applications of fluid mechanics in industry and environment*, ISI Kolkata, India.